Principles of soil water behavior

Nielsen D.R.

in

Kirda C. (ed.), Steduto P. (ed.).
Soil water balance and transport processes: Review of theory and field applications

Bari : CIHEAM
Cahiers Options Méditerranéennes; n. 46

2000
pages 27-66

Donald R. NIELSEN

Department of Land, Air and Water Resources

University of California

DAVIS, CALIFORNIA

USA

PRINCIPLES of SOIL WATER BEHAVIOR

BASIC SOIL WATER CONCEPTS

The liquid phase of a soil is never just pure water. There are always mineral salts and organic substances dissolved in the water. Traditionally in soil physics, solutes were usually neglected except when saline soils were studied. Generally, the liquid phase of soil is called soil water, and today the implications of its solutes are becoming better understood and recognized for the important role they play in water retention and transport in field soils. Here, we shall initially review basic concepts of the forces acting on soil water, soil water potential and soil water retention, and equations to describe soil water movement under water-saturated and unsaturated conditions. Processes of infiltration, evaporation and redistribution of water will be presented for simple initial and boundary conditions occurring within homogeneous soil columns.

Next we consider the physical, chemical and biological processes within a soil profile that distribute, dilute or concentrate solute species within the liquid phase of a soil. The relative concentration of solutes in the liquid phase governs not only the retention and transport of water within soils but also contributes to our understanding of managing the quality of water within soils and that moving below plant roots deeper into the vadose zone. We consider both microscopic and macroscopic considerations of solute behavior in soils.

The processes of soil water behavior and solute transport will be discussed with examples measured in the field. A complete set of references for the material in this chapter is available in Kutílek and Nielsen (1994). Details of methods to measure soil water and soil solutes will be presented in other chapters.

Forces Acting on Soil Water

We begin by studying the system of soil and water in an equilibrium state, characterized by zero fluxes in the soil. The soil water content does not change in time and the water and its solutes are in equilibrium with internal and external forces acting on the system. Although we do not pay attention to the rate at which the equilibrium state was reached, we should know how the equilibrium was obtained. It is usually important to know the recent "history" of the system, e.g. was the equilibrium reached by wetting or drying of the soil? The forces may be grouped according to their nature into separate categories – adsorption, capillarity and swelling.

Adsorption

All three phases – solid, liquid and gas – usually occur simultaneously in almost all soils. Force fields existing at the interfaces of solid-liquid, liquid-gas and solid-gas influence the behavior of soil water. Solutes in the soil water contribute to and modify the action of these force fields. The action between the surface of a solid soil particle including its sorbed ions and water takes place in close proximity of the surface. This portion of soil water is commonly called adsorption water. It can be most easily studied in the absence of other forces and is usually observed when limited amounts of water vapor are adsorbed on the solid soil particles. The adsorptive force field decreases with the distance from the solid surface. In Fig. 1, the adsorbed water can be visualized as thin films covering the soil particle surfaces while capillary water to be discussed next occupies the wedges between the particles.

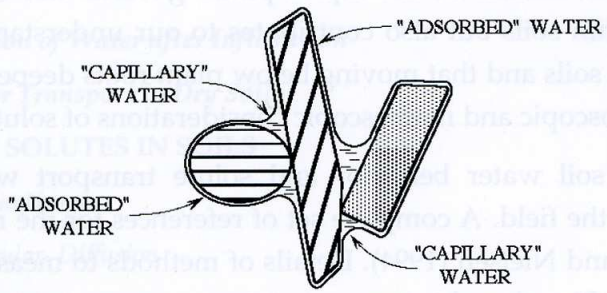

Fig. 1 *- Schematic diagram of adsorbed water and capillary water within soil pores.*

Capillarity

Water filling only parts of the smaller spaces in an unsaturated soil forms curved interfaces between air and water. Capillary forces arise from these interfaces. When water meets a solid surface, a contact angle γ is formed, see Fig. 2. This contact angle is observed when a drop of water is placed on a plane solid surface, or when the solid plate is submerged into water. The magnitude of γ is used to distinguish three classes of wetting for the solid surface. For $\gamma = 0°$, the surface is completely wet and the solid is fully hydrophilic. A non-complete wetting of the surface occurs for $0 < \gamma < 90°$ and the solid is partly hydrophilic. A non-wetting surface exhibits $\gamma \geq 90°$ and the solid is hydrophobic.

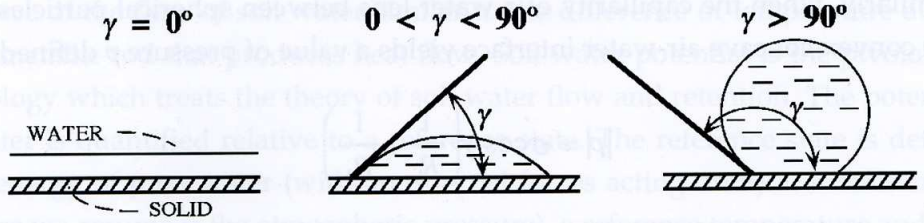

Fig. 2 - Manifestation of the contact angle γ for a liquid on a solid.

Let us assume that the walls of a capillary of radius r are hydrophilic. Water rises into the capillary when its lower end is placed into a pool of water. The height h of this capillary rise is

$$|h| = \frac{2\sigma \cos\gamma}{r\rho_w g} \tag{1}$$

where σ and ρ are the surface tension and density of water, respectively, and g the gravitational acceleration at the earth's surface. For water at 20°C and with $\gamma = 0°$, $|h|$ is approximately equal to $0.15/r$ for length units in cm. Note in Fig. 3 the magnitude of h for the concave meniscus is less than zero. If we installed instruments for measuring the hydrostatic pressure, a straight line passing through zero at the plane water level would be observed. Below the water level, the hydrostatic pressure is positive, and above it in the water column of the capillary, the pressure is negative. The atmospheric pressure is taken as the reference.

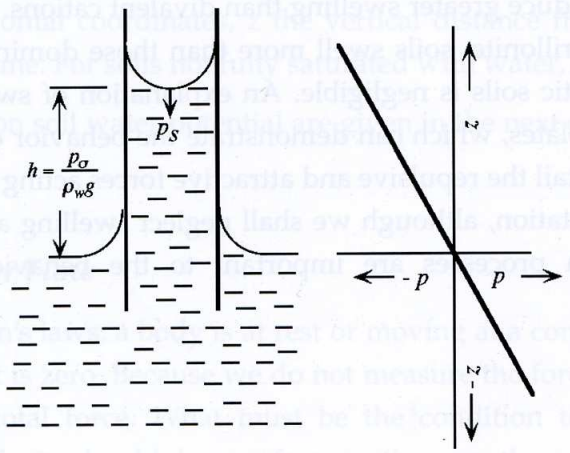

Fig. 3 - Capillary rise for $0° \le \gamma \le 90°$.

Similarly, when the capillarity of a water lens between spherical particles is studied (Fig. 4), the convex-concave air-water interface yields a value of pressure p defined by

$$|p| = \sigma \cos\gamma \left(\frac{1}{R_1} + \frac{1}{R_2} \right) \qquad (2)$$

where R_1 is positive and R_2 is negative. From this discussion it follows that the soil water pressure is negative above the free (ground) water level.

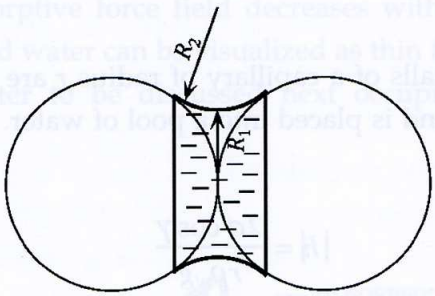

Fig. 4 - A convex-concave air-water interface at the contact of two spherical particles. The water lens has two radii of curvature R_1 *and* R_2.

Swelling

When water penetrates between two parallel clay particle surfaces, the surfaces tend to shift apart - a phenomenon called swelling. Swelling depends upon the clay content, mineralogical composition of clay and upon the exchangeable cations. Monovalent exchangeable cations induce greater swelling than divalent cations. When the clay fraction is dominated by montmorillonite, soils swell more than those dominated by chlorite or illite. The swelling of kaolinitic soils is negligible. An explanation of swelling starts with simple model of two parallel plates, which can demonstrate the behavior of plates of clay. Iwata et al. (1988) describe in detail the repulsive and attractive forces acting upon two parallel plates. In the foregoing presentation, although we shall neglect swelling and shrinkage, it must be remembered that such processes are important to the behavior of water and solute movement in field soils.

Soil Water Potential

The sum of the action of the above forces are all included within the concept of the soil water potential. Generally, the difference of the potential at two separate points relates to the

driving force of the flow of soil water similar to the difference of temperature at the distant ends of a metallic rod that produces heat flow. Soil water potential is the pivotal concept of soil hydrology which treats the theory of soil water flow and retention. The potential energy of soil water is quantified relative to a reference state. The reference state is defined as the potential energy of pure water (with no external forces acting on it) at a reference pressure (which here we assume is the atmospheric pressure), a reference temperature and a reference elevation. Soil water potential is then the potential energy per unit quantity of water relative to the reference potential of zero.

The total potential is the summation of the component potentials

$$\Phi = \phi_g + \phi_w + \phi_o + \phi_a + \phi_e \tag{3}$$

where ϕ_g is the gravitational potential, ϕ_w the soil water potential, ϕ_o the osmotic potential, ϕ_a the pneumatic potential and ϕ_e envelope potential.

In the majority of situations the simplest definition of the total potential is

$$\Phi = \phi_w + \phi_g \tag{4}$$

and with the potential expressed as energy per unit weight of water

$$\Phi = gh(x,y,z,t) + gz \tag{5}$$

the total head H is simply

$$H = h(x,y,z,t) + z \tag{6}$$

where x and y are horizontal coordinates, z the vertical distance from the reference level, positive upwards and t time. For soils not fully saturated with water, $h < 0$.

Further discussions on soil water potential are given in the next chapter (Hartmann, this volume).

Conditions of No Water Flow

According to Newton's laws, a body is at rest or moving at a constant velocity when the sum of forces acting on it is zero. Because we do not measure the forces acting on soil water, we must calculate the total force. What must be the condition to have no flow in the horizontal directions? There should be no force acting on the water in the horizontal directions. Hence, the partial derivatives of Eq. 5 with respect to both x and y must each be identically zero. In other words,

$$F = -\frac{\partial \Phi}{\partial x} = -g\frac{\partial h}{\partial x} = 0 \qquad F = -\frac{\partial \Phi}{\partial y} = -g\frac{\partial h}{\partial y} = 0 \tag{7}$$

Inasmuch as g is not zero, the values of h must be constant in both directions.

What must be the condition to have no flow in the vertical direction? There should be no force acting on the water in the vertical direction. Hence, the partial derivative of Eq. 9 with respect to z must be identically zero.

$$F = -\frac{\partial \Phi}{\partial z} = -g\frac{\partial h}{\partial z} - g\frac{\partial z}{\partial z} = -g\left(\frac{\partial h}{\partial z} + 1\right) = 0 \tag{8}$$

Because the parenthetic value must be nil,

$$h = -z + c \tag{9}$$

where c is a constant of integration. When no water flows vertically, the values of h and z throughout the soil must equal but opposite in sign.

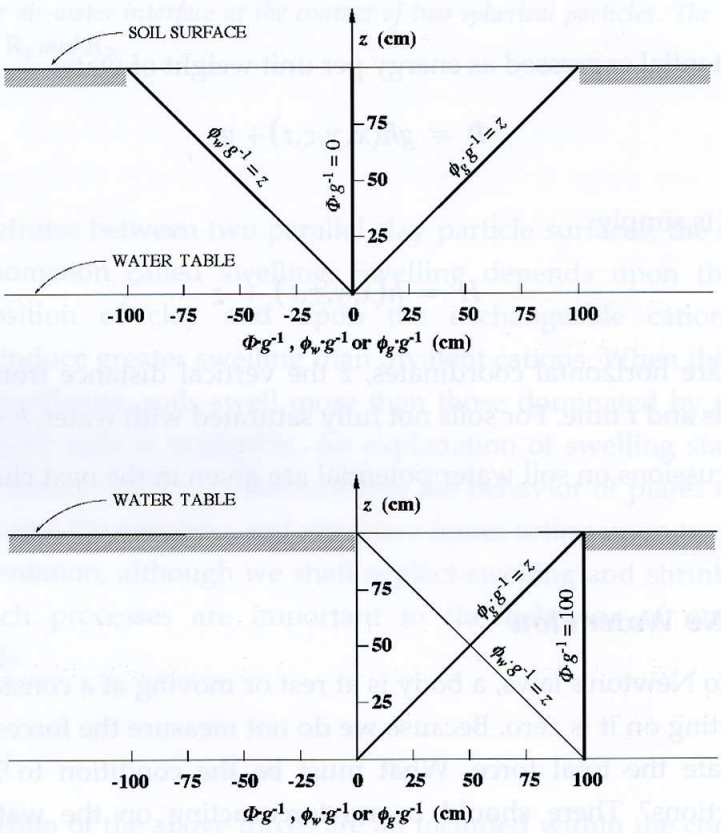

Fig. 5 - Vertical potential distributions for two stagnant flow conditions.

Two examples are illustrated in Fig. 5 when water tables exist at a soil depth of 100 cm and at the soil surface. Note that under the wetter condition with the water table at the soil surface the magnitude of the total potential Φ is greater, but its derivative remains nil.

Rate of Soil Water Flow

The rate at which water moves through a soil is proportional to the force acting on the water,

$$\bar{q} \ \alpha \ \bar{\nabla}\Phi \tag{10}$$

where $\bar{q}$ is the flux density vector equal to the volume of water moving per unit time through a unit surface area normal to the direction of flow. If we consider the flux density in only the vertical direction, Eq. 10 becomes

$$q \ \alpha \ -\frac{d\Phi}{dz} = -g\frac{d\left(\phi_w \cdot g^{-1} + \phi_g \cdot g^{-1}\right)}{dz} \tag{11}$$

or

$$q \ \alpha \ -g\frac{d(h+z)}{dz} = -g\left(\frac{dh}{dz}+1\right). \tag{12}$$

If we assume the flux density q and the force given by the last term in Eq. 12 are related equal by a constant for a particular value of h or θ, we have the Darcy-Buckingham equation

$$q = -K\left(\frac{dh}{dz}+1\right) \tag{13}$$

where the hydraulic conductivity K equals $k\gamma g\mu^{-1}$ with k being the intrinsic permeability reflecting the geometry of the soil pores, and γ and μ the density and viscosity of the soil water, respectively.

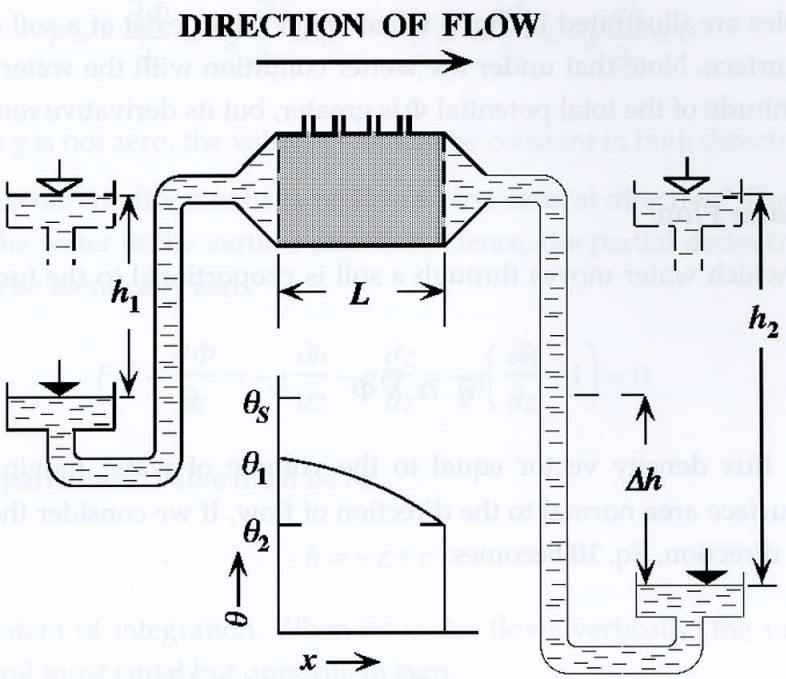

Fig. 6 - A simple steady flow experiment on an unsaturated soil column.

A simple example of unsaturated flow is demonstrated in Fig. 6. The cylinder containing the soil has small openings within its walls leading to the atmosphere. Semipermeable membranes, permeable to water but not to air, separate the soil from free water on both sides of the cylinder. The pools of water are connected to the cylinder with flexible tubes. Full saturation of the soil is first achieved when both pools, lifted to the highest point of the soil, displace the soil air through the openings on the top side of the cylinder. At this moment, there is no flow in the system and the soil is assumed water saturated. With the pool on the left side of the cylinder lowered to the position h_1 and the pool on the right side to position h_2, air enters into the soil through the openings as the soil starts to drain in a manner similar to a soil placed on a tension plate apparatus. Although water flows from the left pool to the right pool, the rate of flow is reduced significantly compared with that when the soil is water saturated. If the water level in each of the pools is kept at a constant elevation with time, steady flow will eventually be reached with the water content at each point within the soil remaining invariant. At this time, the flux density q will depend upon the hydraulic gradient and be governed by an equation similar to Eq. 13 with the force of gravity omitted because water is flowing only horizontally with the gravitational head being every where the same

$$q = -K(h)\frac{dh}{dx} \tag{14}$$

Inasmuch as the soil is not water saturated and flow occurs primarily in those pores filled with water, the value of K will be smaller than that of the saturated hydraulic conductivity K_S for the same soil. The unsaturated hydraulic conductivity K $[h(\theta)]$ is physically dependent upon the soil water content θ because water flow is realized primarily in pores completely filled with water. Coarse-textured soils generally have greater values of K than those of fine-textured soils near water saturation ($-h \rightarrow 0$). On the other hand, fine-textured soils usually have the greater values as the value of h diminishes. See Fig. 7.

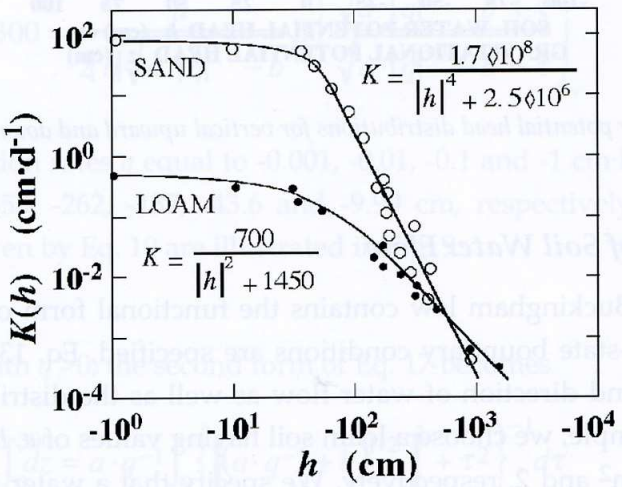

Fig. 7 - Measured values of K(h) *for a sand and a loam (Willis, 1960).*

The experimantal values of K satisfy the empirical relation

$$K = \frac{a}{|h|^n + b} \tag{15}$$

where a, b and n are constants. Values of n for clays are about 2 while those for sands are 4 or greater. Note that when $h \geq 0$ in Eq. 15 the ratio of a and b is the value of the saturated hydraulic conductivity K_S.

Direction of Soil Water Flow

The direction of vertical flow depends upon the magnitude and sign of the derivative of h compared to 1 in Eq. 13 where vertical soil depth was measured positively upward with reference to water table depth. For $q > 0$, water flows upward and for $q < 0$, water flows downward. See Fig. 8.

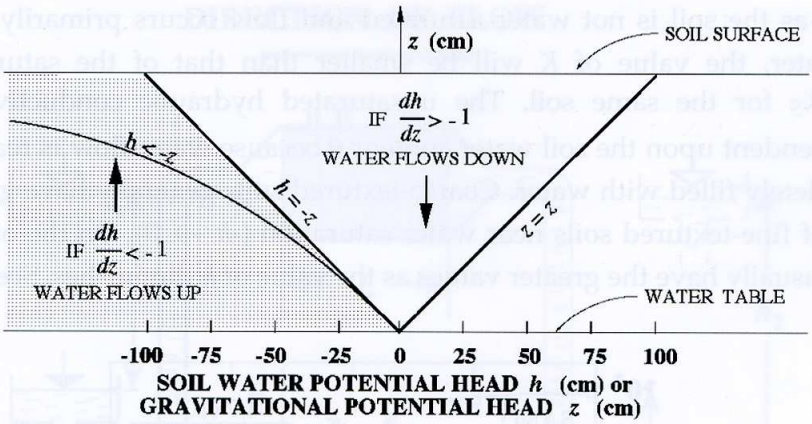

Fig. 8 - Soil water potential head distributions for vertical upward and downward water flow.

Rate and Direction of Soil Water Flow

When the Darcy-Buckingham law contains the functional form of $K(h)$ for a particular soil, and if the steady-state boundary conditions are specified, Eq. 13 may be integrated to yield the magnitude and direction of water flow as well as the distribution $h(z)$ within the soil profile. As an example, we choose a loam soil having values of a, b and n in Eq. 15 equal to 200 $cm^3 \cdot hr^{-1}$, 100 cm^2 and 2, respectively. We specify that a water table exists at the 3-m depth. If we specify the flux density, we may calculate the distribution $h(z)$. To avoid complications of signs, we shall select $\tau = -h$ where τ is always positive in our calculations. Hence, we designate the total potential head $H = (\tau + z)$ with the reference level for gravitational potential being zero at the water table $z = 0$.

Substituting Eq. 15 into Eq. 13 and integrating with respect to the above boundary conditions, we have

$$\int_0^{300} dz = \int_0^{\tau} \frac{d\tau}{1 + q \cdot K^{-1}(\tau)} = \frac{a}{q} \int_0^{\tau} \left[\left(a \cdot q^{-1} + b \right) + \tau^2 \right]^{-1} d\tau \qquad (16)$$

Note that if q is known, the equation can be solved for its only unknown quantity τ at the soil surface. On the other hand if τ is specified, the value of q can be calculated.

Depending on the sign of q, and the relative magnitudes of a and b, the integral in Eq. 19 is of the form

$$\int \frac{du}{c^2 - u^2} = \frac{1}{2c} \ln \left(\frac{c+u}{c-u} \right) \text{ or } \int \frac{du}{c^2 + u^2} = \frac{1}{c} \tan^{-1} \frac{u}{c} . \qquad (17)$$

For infiltration with $q < 0$, the first form is appropriate and becomes

$$\int_0^{300} dz = a \cdot |q|^{-1} \int_0^{\tau} \left\{ \left[\left(a \cdot |q|^{-1} - b \right)^{1/2} \right]^2 - \tau^2 \right\}^{-1} d\tau \tag{18}$$

Upon integration, Eq. 18 becomes

$$300 = \frac{a}{2|q|\sqrt{a \cdot |q|^{-1} - b}} \ln \left(\frac{\sqrt{a \cdot |q|^{-1} - b} + \tau}{\sqrt{a \cdot |q|^{-1} - b} - \tau} \right) \tag{19}$$

For steady infiltration rates q equal to -0.001, -0.01, -0.1 and -1 cm·hr^{-1}, the values of h at the soil surface are -355, -262, -137, -43.6 and -9.99 cm, respectively. The corresponding distributions of $z(h)$ given by Eq. 19 are illustrated in Fig. 9.

For evaporation with $q > 0$, the second form of Eq. 17 becomes

$$\int_0^{300} dz = a \cdot q^{-1} \int_0^{\tau} \left\{ \left[\left(a \cdot q^{-1} + b \right)^{1/2} \right]^2 + \tau^2 \right\}^{-1} d\tau \tag{20}$$

and upon integration is

$$300 = \frac{a}{q\sqrt{a \cdot q^{-1} + b}} \tan^{-1} \left(\frac{\tau}{\sqrt{a \cdot q^{-1} + b}} \right) \tag{21}$$

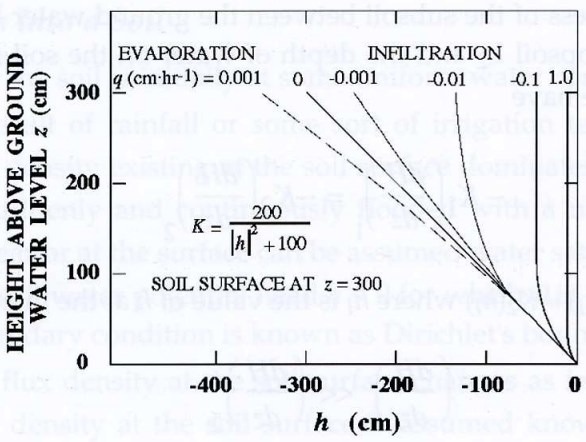

***Fig. 9** - Soil water potential head distributions for steady state evaporation, no flow and infiltration.*

The distribution by Eq. 21 is given in Fig. 9 for an evaporation rate q = 0.001 cm·hr^{-1}. At that rate, the value of h at the soil surface is -355 cm. We note that a maximum evaporation rate of 0.00547 cm·hr^{-1} is reached by allowing the value of h at the soil surface to decrease and approach -∞. Integrating Eq. 16 for other soils (n = 3, 4, 5 etc.) for soils that are progressively more sandy, it can be easily shown that the maximum rate of evaporation is proportional to L^{-n} where L is the depth of the water table.

Steady Infiltration into a 2-Layered Soil

The simplest case is the crust-topped profile. Rainfall frequently destroys soil aggregates within a soil surface. Tillage also induces compaction. Both processes often denoted by sealing, crusting or compaction results in the formation of a less permeable soil surface layer. The characteristics of the topsoil will be denoted by the index 2, while those of the subsoil will be given the index 1, see Fig. 10.

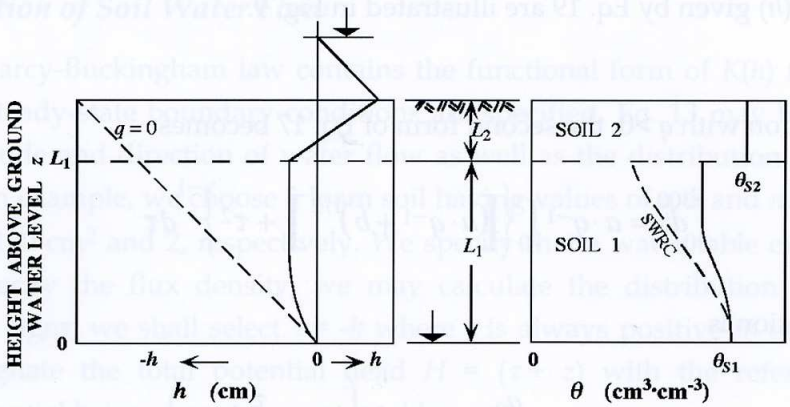

Fig. 10 *- Steady flow infiltration into a two-layered soil.*

The origin of the z-axis is identical with the position of the ground water level which is kept constant. The thickness of the subsoil between the ground water level and the topsoil is L_1, the thickness of the topsoil L_2 and the depth of water on the soil surface h_o. For steady-state flow, $q_1 = q_2$, and we have

$$-K_1\left(\frac{dH}{dz}\right)_1 = -K_2\left(\frac{dH}{dz}\right)_2 . \qquad (22)$$

If $K_{S1} \gg K_{S2}$, and $K_1(h_I) \gg K_2(h_I)$ where h_I is the value of h at the interface, we have

$$\left(\frac{dH}{dz}\right)_1 \ll \left(\frac{dH}{dz}\right)_2 \qquad (23)$$

and because $H = (h + z)$,

$$\left(\frac{dh}{dz}\right)_1 << \left(\frac{dh}{dz}\right)_2 \tag{24}$$

This condition of a larger gradient of h occurring in the topsoil (layer 2) demands a sufficiently small value of h_I including $h_I < 0$. Because we assume that just below the interface in the subsoil (layer 1), $dH/dz \approx 1$, we can write

$$q = - K_1(h_I) \tag{25}$$

For the topsoil assuming it remains water-saturated,

$$q = - K_{S2}\left(\frac{h_o - h_I + L_2}{L_2}\right) \tag{26}$$

The value of h_I is obtained by equating Eq. 25 and Eq. 26. The subsoil can be unsaturated if $|q| < K_{S1}$. Under the assumptions here, the subsoil becomes unsaturated below the topsoil when

$$h_o < L_2\left(\frac{K_{S1}}{K_{S2}} - 1\right) \tag{27}$$

For more general conditions than those assumed here, the bottom of the topsoil above the interface can also become unsaturated. For such cases, the above approach has to be modified, see e.g. Takagi (1960) and Srinilta et al. (1966).

Unsteady Infiltration into a Soil

Let us assume that the soil is initially at some uniform water content θ_n. Water can enter the soil surface as a result of rainfall or some sort of irrigation technique. The soil water potential or water flux density existing at the soil surface dominates the infiltration process. If the soil surface is suddenly and continuously flooded with a negligibly small depth of water ($h = 0$), the soil near or at the surface can be assumed water saturated. It is also possible to maintain a constant soil water potential head $h < 0$ for which θ is maintained constant and less than θ_S. Such a boundary condition is known as Dirichlet's boundary condition. For such a condition, the water flux density at the soil surface changes as infiltration occurs. On the other hand, if the flux density at the soil surface is assumed known, Neuman's boundary condition exists. It can describe constant rainfall at rates less than as well as greater than K_S,

and nonconstant rainfall. It also is appropriate for controlled sprinkler and other flux controlled techniques for applying water to the soil surface. Here we give a couple of examples using only the Dirichlet condition.

The primary infiltration data usually measured are values of cumulative infiltration I (cm) as a function of time. The values represent the total amount of water infiltrated into the soil from the beginning of the infiltration test at $t = 0$. A typical $I(t)$ relationship (Fig. 11) is a smooth, monotonically rising curve.

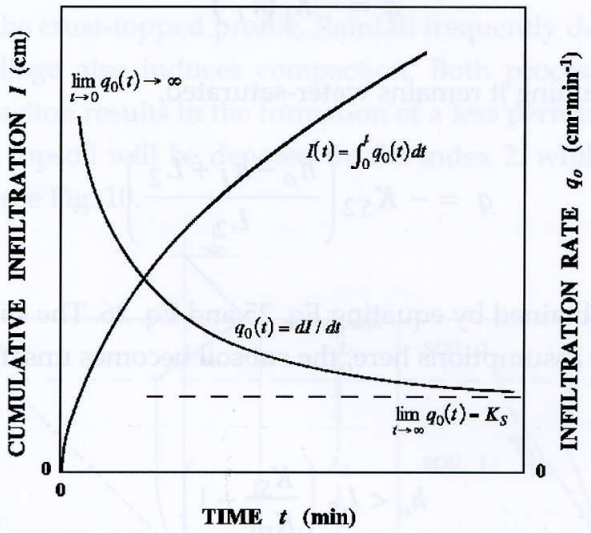

Fig. 11 - Time dependence of cumulative infiltration and infiltration rate

The infiltration rate $q_o = dI/dt$ where the subscript o refers to the soil surface at $z = 0$. The value of q_o initially decreases rapidly with time and eventually approaches a constant value. For $t = 0$, $q_o \to \infty$, and for $t \to \infty$, q_o = constant. Theoretically, $q_o \to K_S$ as $t \to \infty$. Practically, the infiltration rate starts to be constant for coarse textured soils after only decades of minutes while that for fine textured loams is in the order of hours, depending upon the hydraulic functions of the soil and θ_n.

When unsteady soil water flow exists, two equations are needed to describe the water flux density and the rate of change of soil water content in time. The flux density described by the Buckingham-Darcy equation and the rate of filling or emptying of the soil pores described by the equation of continuity are combined into the Richards' equation

$$\frac{\partial \theta}{\partial t} = \frac{\partial}{\partial z}\left[K(h)\frac{\partial h}{\partial z}\right] - \frac{\partial K}{\partial z} \qquad (28)$$

for vertical, one-dimensional flow where z is measured positively in the downward direction.

If the soil is only wetting, θ will be uniquely dependent upon only h and

$$\frac{\partial h}{\partial z} = \frac{dh}{d\theta}\frac{\partial \theta}{\partial z} \tag{29}$$

which leads to the diffusivity form of Richards' equation

$$\frac{\partial \theta}{\partial t} = \frac{\partial}{\partial z}\left[D(\theta)\frac{\partial \theta}{\partial z} \right] - \frac{\partial K}{\partial z} \tag{30}$$

where the Darcy-Buckingham equation has the diffusivity form

$$q = - D(\theta)\frac{\partial \theta}{\partial z} - K(\theta) \tag{31}$$

and the soil water diffusivity D is the term derived from

$$D(\theta) = K(\theta)\frac{dh}{d\theta}. \tag{32}$$

The main reason for the derivation of Eq. 30 is the reduction of the number of variables from 4 to 3.

The first term on the right hand side of Eq. 30 accounts for the forces associated with differences of the soil water potential as illustrated in Fig. 5. The second term on the right hand side of Eq. 30 accounts for the gravitational force because water is moving vertically. During early stages of infiltration the second term is negligible, and during late stages it dominates the process. Hence, here we shall first neglect it and assume water flows horizontally not influenced by gravity, and later consider its influence.

Our horizontal soil column, initially at an unsaturated water content θ_n, has its end at $x = 0$ maintained at water saturation θ_S. Hence, for

$$t \geq 0 \qquad x = 0 \qquad \theta = \theta_S \tag{33}$$

$$t = 0 \qquad x > 0 \qquad \theta = \theta_n \tag{34}$$

we solve Eq. 30 without the gravitational term

$$\frac{\partial \theta}{\partial t} = \frac{\partial}{\partial x}\left[D(\theta)\frac{\partial \theta}{\partial x} \right]. \tag{35}$$

It is only here for a homogeneous soil (i.e. not layered) that the gradient of θ represents the driving force of the process. Here when D is a function of θ, we must transform Eq. 35 into an ordinary differential equation using the Boltzmann transformation.

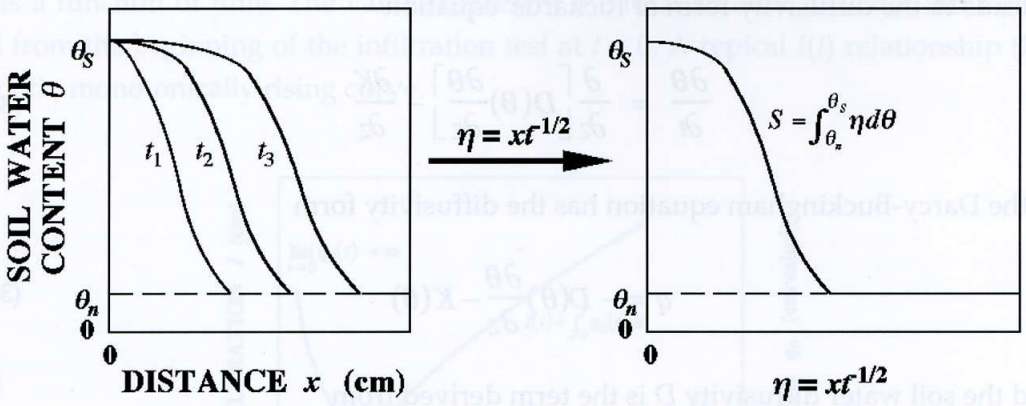

Fig. 12 - Boltzmann's transformation reduces the soil water content profiles θ(x) *into a unique profile* θ(η) *for horizontal infiltration.*

The transformed equation has a new variable η instead of the two original variables x and t. The new variable η defined by the Boltzmann transformation

$$\eta(\theta) = x t^{-1/2} \tag{36}$$

transforms Eq. 38 to

$$-\frac{\eta}{2}\frac{d\theta}{d\eta} = \frac{d}{d\eta}\left[D(\theta)\frac{d\theta}{d\eta}\right] \tag{37}$$

with transformed boundary conditions

$$\eta = 0 \qquad \theta = \theta_S \tag{38}$$

$$\eta = \infty \qquad \theta = \theta_n. \tag{39}$$

The solution for which we search is simply $\theta(\eta)$, see Eq. 36 and Fig. 12. Measured soil water profiles $\theta[x(t_1)]$, $\theta[x(t_2)]$, $\theta[x(t_3)]$ etc. are thus transformed into the unique $\theta(\eta)$ relationship by merely dividing x by $t_1^{1/2}$ for the first profile, $t_2^{1/2}$, for the second profile etc. Note that for $t = 1$, $x \equiv \eta$. Hence, the physical reality of $\theta(\eta)$ is the soil water profile $\theta(x)$ when the infiltration time is unity.

The amount of water infiltrated into the profile is

$$I = \int_{\theta_n}^{\theta_s} x \, d\theta \tag{40}$$

or with Eq. 36,

$$I = \int_{\theta_n}^{\theta_s} \eta(\theta)\, t^{1/2} \, d\theta \tag{41}$$

With the sorptivity S being defined as

$$S = \int_{\theta_n}^{\theta_s} \eta(\theta) \, d\theta \tag{42}$$

we have the cumulative infiltration

$$I = S\, t^{1/2} \tag{43}$$

Because the infiltration rate

$$q_o = dI / dt, \tag{44}$$

we also have

$$q_o = \frac{1}{2} S\, t^{-1/2} \tag{45}$$

Here, we note that the sorptivity is physically the cumulative amount of water infiltrated at $t = 1$, and at that time, the infiltration rate has diminished to one-half the value of S. Sorptivity depends not only upon the $D(\theta)$ function but upon θ_n. The value of S decreases with increasing θ_i and as $\theta_i \rightarrow \theta_S$, $S \rightarrow 0$.

Sorptivity is an integral part of most investigations describing vertical infiltration as we shall learn below.

The solution of Eq. 30 subject to Eq. 33 and Eq. 34 for vertical infiltration is

$$z(\theta,t) = \eta(\theta) t^{1/2} + \chi(\theta) t + \psi(\theta) t^{3/2} + \cdots + f_i(\theta)\, t^{i/2} \tag{46}$$

The cumulative infiltration I is

$$I = S\,t^{1/2} + (A_2 + K_n)t + A_3 t^{3/2} + \cdots + A_i t^{1/2} \tag{47}$$

where K_n is $K(\theta_n)$. Note that $K_n t$ expresses the cumulative water flow with dH/dz = -1 at $\theta = \theta_n$. The series Eq. 47 converges for short and intermediate times of infiltration and the infiltration rate $q_o(t)$ obtained by differentiation is

$$q_o = \frac{1}{2} S\,t^{-1/2} + (A_2 + K_n) + \frac{3}{2} A_3 t^{1/2} + \cdots + \frac{i}{2} A_i t^{i/2-1} \tag{48}$$

For large times, Eq. 47 does not converge. Inasmuch as the shape of the wetting front remains invariant at large times, the wetting front moves downward at a rate

$$v = \left(\frac{K_S - K_n}{\theta_S - \theta_n} \right) \tag{49}$$

while the infiltration rate for $t \rightarrow \infty$ is

$$q_o = K_S \tag{50}$$

Soil water content profiles measured at three different infiltration times in the laboratory for a homogeneous column of Columbia silt loam are given in Fig. 13. The solid lines are calculated using measured values of $K(\theta)$ and $D(\theta)$ in the above equations. The extra depth to which the soil water profile advances owing to the force of the gravitational field is illustrated in Fig. 14 where the distance to the wetting front for horizontal and vertically downward flows are plotted against the square root of time.

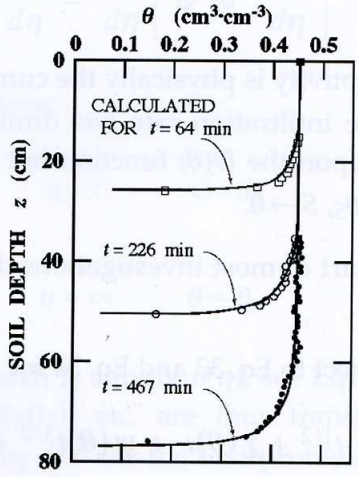

Fig. 13 - Measured and calculated soil water content profiles in Columbia silt loam for a Dirichlet boundary condition.

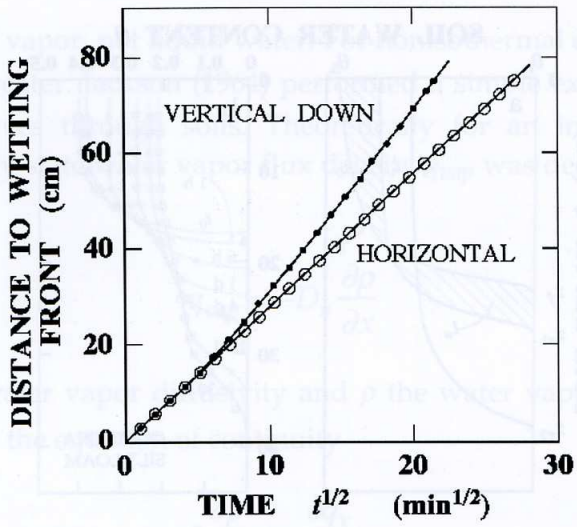

Fig. 14 - Distance to the wetting front versus square root of time for vertical and horizontal infiltration into Columbia silt loam.

During the first 25 min, the depths of wetting for both horizontal and vertical infiltration are nearly identical. After 400 min, the vertical profile is more than 12 cm deeper than that of the horizontal profile, and the infiltration rate is nearly constant and equal to K_S according to Eq. 50.

Redistribution of Water after Infiltration

After infiltration ceases, the soil water content gradually decreases even when the soil surface is protected by a cover allowing no evaporation. The decrease of θ within the originally wetted topsoil is caused by a downward flow of soil water. When water draining from the wetted topsoil wets the originally drier subsoil, we speak of soil water redistribution. At that time a relatively large soil water potential frequently near $h = 0$ exists within the topsoil down to the depth of the wetting front z_f. Below the wetting front, the value of h is very small, and hence, the soil water profile is in a dynamic state rather than one of equilibrium. When we discuss this non-equilibrium process caused by infiltration, we denote the time of cessation of infiltration $t_o = 0$. The non-equilibrium condition produces a downward water flux within the soil profile without a contribution to the flux from the surface, i.e. at $z = 0$, $\theta_o = 0$. With the soil between $z = 0$ and $z = z_f$ being drained, water flows below z_f forming a new redistribution wetting front at z_r, see Fig. 15a.

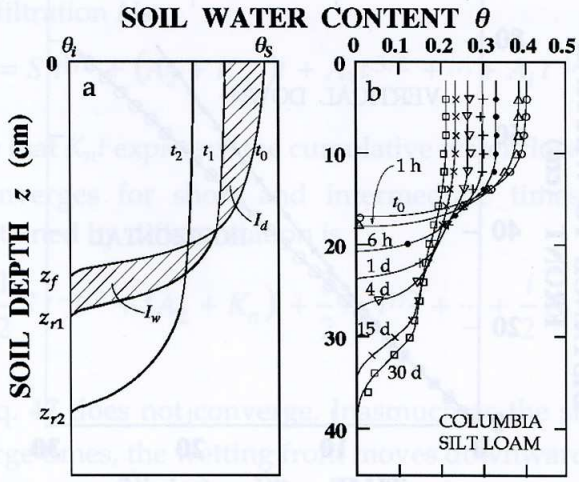

Fig. 15 - Conceptual and measured soil water content profiles during redistribution after infiltration.

The soil water content profile $\theta(z)$ at t_o is the profile at the end of infiltration. Subsequently, at times t_1, t_2, t_3, ···, redistribution profiles are observed. The cumulative drainage I_d and the cumulative wetting I_w below z_f are equal for the time interval $(0, t_1)$, see the hatched areas in Fig. 15a. The rate of movement depends upon the hydraulic conductivity and the depth of the original wetting front from the infiltration. The flux density across the redistribution front decreases in time owing to two factors. First, the potential in the wetted topsoil decreases with a simultaneous decrease of the gradient of the total potential dH/dz. Second, the value of the hydraulic conductivity decreases strongly with only slight decreases of θ.

Soil water profiles during redistribution in Columbia silt loam given in Fig. 15b resemble those in Fig. 15a. At time t_0, 6.1 cm of water had just infiltrated the soil surface with the wetting front reaching 17 cm. Soil water contents near the soil surface decrease gradually and uniformly by developing zones of nearly constant water content extending from the soil surface downward. After 30 d of redistribution, the wetting front has reached nearly 40 cm and the water content at the soil surface has diminished to 0.21 $cm^3 \cdot cm^{-3}$. At that time the initially abrupt wetting front into the dry soil is no longer evident, indicative of water movement at extremely small water contents. Other measurements of redistribution in Columbia silt loam showed that rate of redistribution is inversely related to the initial depth of wetting which is just the opposite for sands.

Water Vapor Transport in Dry Soils

In relatively dry soils when a great portion of the pores are filled with air and liquid water exists in very thin layers on the soil particle surfaces, the flux density of water is

composed primarily of vapor, not liquid water. For nonisothermal conditions, the transfer of water vapor is even greater. Jackson (1964) performed a simple experiment to demonstrate how water vapor moves through soils. Theoretically for an inert porous medium, he assumed that the steady state water vapor flux density q_{vap} was described by Fick's first law of diffusion

$$q_{vap} = -D_v \frac{\partial \rho}{\partial x} \tag{51}$$

where D_v is the soil water vapor diffusivity and ρ the water vapor density in the soil air. Combining Eq. 51 with the equation of continuity

$$\varepsilon \frac{\partial \rho}{\partial t} = -\frac{\partial q_v}{\partial x} \tag{52}$$

we have for transient conditions in an inert medium

$$\varepsilon \frac{\partial \rho}{\partial t} = \frac{\partial}{\partial x}\left(D_v \frac{\partial \rho}{\partial x} \right) \tag{53}$$

where ε is the air-filled porosity. Because soil is not inert, it can absorb the water vapor and have it condense on its particles' surfaces as well as the reverse - contribute to the vapor density of its air-filled pores from the liquid water on its particle surfaces. At equilibrium the adsorption isotherm $\rho(\theta)$ expresses the relation between the water in the soil air to that in the liquid state. Recognizing that ρ is a function of the soil water content θ, Eq. 51 becomes

$$q_{vap} = -D_v \frac{d\rho}{d\theta} \frac{\partial \theta}{\partial x} = -D_{\theta vap} \frac{\partial \theta}{\partial x} \tag{54}$$

where $D_{\theta vap}$ is the product of D_v and the slope of the vapor adsorption isotherm $\rho(\theta)$. For a soil, Eq. 53 becomes

$$\varepsilon \frac{\partial \rho}{\partial t} = \frac{\partial}{\partial x}\left(D_{\theta vap} \frac{\partial \theta}{\partial x} \right) - \frac{\partial \theta}{\partial t} \tag{55}$$

where the second term on the right-hand side of Eq. 55 accounts for the water vapor being adsorbed on the soil and changing the soil water content θ. If

$$\varepsilon \frac{\partial \rho}{\partial t} << \frac{\partial \theta}{\partial t},$$

Eq. 55 becomes

$$\frac{\partial \theta}{\partial t} = \frac{\partial}{\partial x}\left[D_{\theta vap}(\theta) \frac{\partial \theta}{\partial x} \right] \tag{56}$$

which is identical in form to Eq. 35. By only measuring soil water contents within a soil column, a separation of that water moving as vapor and that as liquid cannot be achieved. Hence, we rewrite Eq. 56 as

$$\frac{\partial \theta}{\partial t} = \frac{\partial}{\partial x}\left[D_{\theta v}(\theta) \frac{\partial \theta}{\partial x} \right] \tag{57}$$

where $D_{\theta v}$ accounts for both vapor and liquid transfers and is defined as

$$D_{\theta v}(\theta) = D_{\theta vap} + D_{\theta liq} . \tag{58}$$

Jackson used pressure dependence of $D_{\theta vap}$ to ascertain the relative magnitudes of $D_{\theta vap}$ and $D_{\theta liq}$.

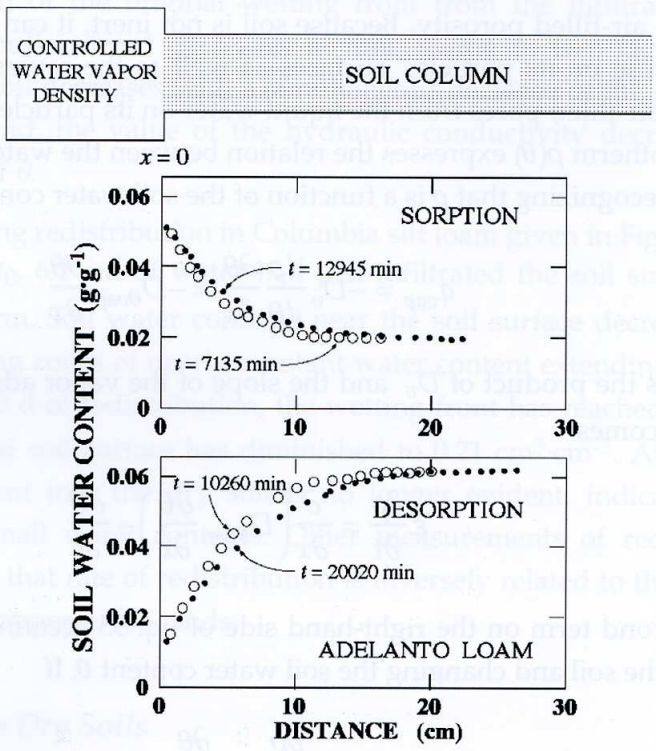

Fig. 16 *- Experimental apparatus to observe water vapor transport and measured soil water content profiles for two different times of sorption and desorption, respectively.*

The experimental set-up to study water vapor diffusion is shown at the top of Fig. 16. A homogeneous soil initially at water content θ_n was subjected to a constant vapor density at $x = 0$. The constant vapor density at $x = 0$ gives rise to a constant soil water content θ_0 If $\theta_0 > \theta_n$, the soil absorbs water. If $\theta_0 < \theta_n$, the soil loses water.The top graph in Fig. 16 shows soil water content profiles of a soil having $\theta_n = 0.02$ g·g^{-1} and being subjected to $\theta_0 = 0.05$ g·g^{-1} for times of 7,135 and 12,945 min (about 5 and 9 d). Water moves into these soil columns. The bottom graph in Fig. 16 shows soil water content profiles of a soil having $\theta_n = 0.06$ g·g^{-1} and being subjected to $\theta_0 = 0.01$ g·g^{-1} for times of 10,260 and 20,020 min (about 7 and 14 d). Water moves out of these soil columns.

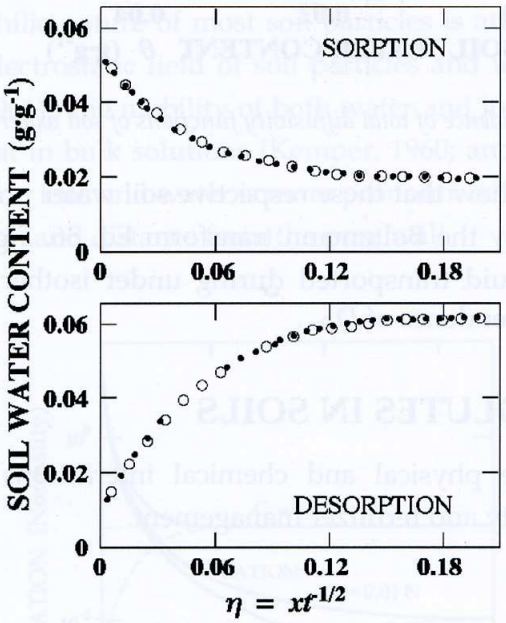

Fig. 17 - Soil water content profiles of Fig. 16 scaled with Boltzmann transformation.

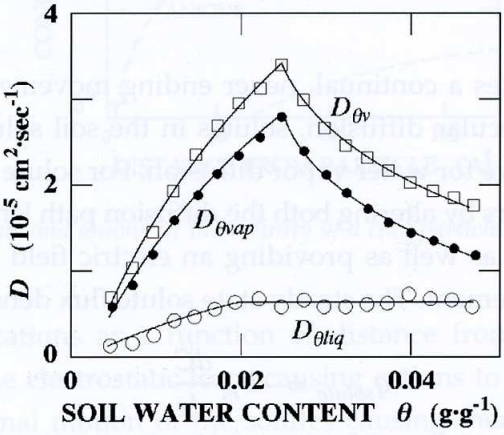

Fig. 18 - Total, vapor and liquid diffusivity functions of soil water content for 25° C for Adelanto loam.

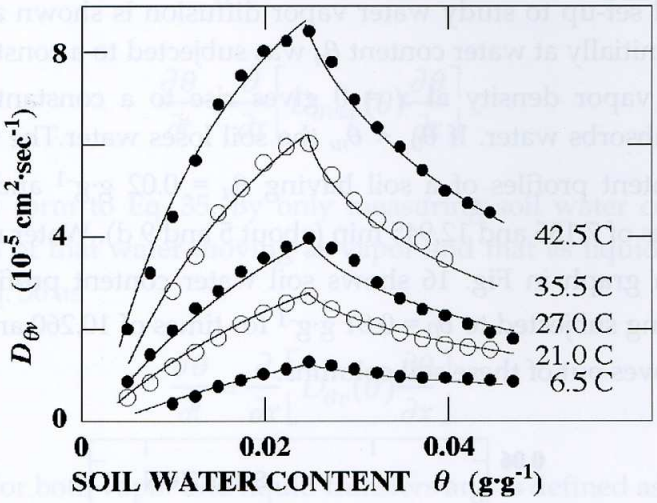

Fig. 19 *- Temperature dependence of total diffusivity functions of soil water content for Adelanto loam.*

The graphs in Fig. 17 show that these respective soil water profiles at different times are coalesced into one curve by the Boltzmann transform Eq. 36. Figure 18 shows the relative amounts of vapor and liquid transported during under isothermal conditions. Figure 19 shows the temperature dependence of $D_{\theta v}$.

TRANSPORT OF SOLUTES IN SOILS

First we consider the physical and chemical interactions of solutes that play an important role in soil salinity and fertilizer management.

Solute Interactions

Molecular Diffusion

Thermal energy provides a continual, never ending movement of liquid phases of the soil system. Owing to molecular diffusion, solutes in the soil solution obey Fick's first law similar to that of Eq. 51 above for water vapor diffusion. For solute diffusion, the solid matrix of the soil complicates matters by altering both the diffusion path length and the cross sectional area available for diffusion as well as providing an electric field and reactive surfaces that further alter molecular movement. The steady state solute flux density is given by

$$q_{solute} = -D_m \frac{dC}{dx} \tag{59}$$

where D_m is the molecular diffusion coefficient and C the concentration of the solute.

Electric Force Fields

Electric force fields always exist within the pore structure of soils owing to the electric charge possessed by the walls of soil pores. The charge per unit pore wall area is caused by isomorphous substitution of atoms in the tetrahedral and octahedral layers of the clay minerals as well as the presence of the Si-O-H (silanol) group on quartz, kaolin minerals and other surfaces like organic matter (-OH and -COOH). The magnitude of the former is fixed while that of the latter depends upon pH and concentration of the soil solution. In general, small highly charged ions cause the viscosity of the soil solution to increase while large monovalent ions cause the viscosity to decrease. The electrostatic fields of the ions cause polarization and a binding of surrounding water molecules which alter the kinetic properties of soil water. The hydrophilic nature of most soil particles is attributed to the attraction of hydrated cations by the electrostatic field of soil particles and to the hydrogen bonding of water to the clays (Low, 1961). The mobility of both water and ions in the region of the pore walls is reduced below that in bulk solutions (Kemper, 1960; and Dutt and Low, 1962). The impact of the electric field on ions and water is more pronounced in clayey soils and depends upon the ionic concentration and distance from the pore wall.

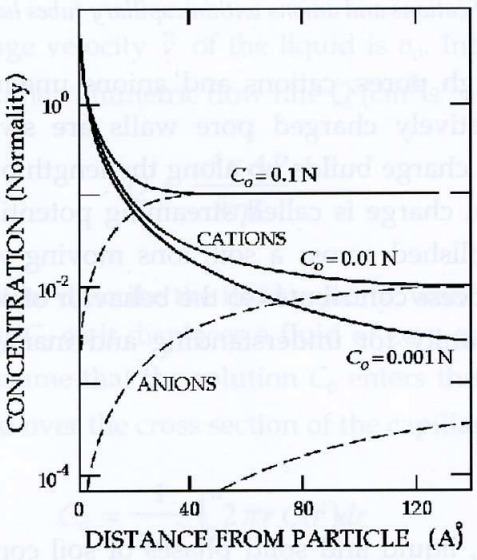

***Fig. 20** - Distributions of cations and anions in the vicinity of a clay particle surface for three diferent solution concentrations.*

The distribution of cations as a function of distance from a negatively charged flat surface is explained by the electrostatic force causing cations to move toward the surface is counteracted by the thermal motion of the solutes causing them to diffuse away from the surface. We see in Fig. 20 that the extent of the unequal distribution of cations and anions

away from the surface depends inversely upon the total concentration C_o of the solution. And, we note from Fig. 21 for cylindrical pores with a wall having a net negative charge and filled with a solution of concentration C_o that the concentration distribution across the pores depends upon the magnitude of the pore radius. In the center of large pores the concentrations of cations and anions are identical while in the center of small pores owing to the electric field, the cationic concentration exceeds that of anions.

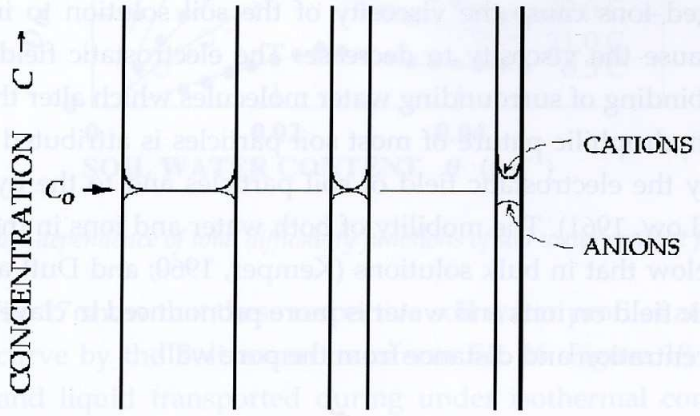

***Fig. 21** - Distributions of cations and anions within capillary tubes having three different radii.*

As water moves through pores, cations and anions unequally distributed across the pores because of the negatively charged pore walls are swept along with the water. Consequently, a differential charge builds up along the length of flow which tends to retard water flow. This differential charge is called streaming potential. Similarly, if an electrical potential difference is established across a soil, ions moving within the electric field will create a water flux. Each process contributes to the behavior of solutes and water at the pore scale and offers an opportunity for understanding and managing solute movement and retention in soil profiles.

Other Interactions

Constituents in the gas, liquid and solid phases of soil continually reacting with each other through a variety of chemical and biological pathways contribute to the presence and behavior of particular solutes in soil profiles. Applicable equilibrium and nonequilibrium chemical concepts are those of oxidation-reduction, solubility-precipitation, association-dissociation, acid-base and exchange-adsorption. Microbiological reactions as well as those involving root systems of higher plants contribute to the behavior of solutes in field soils. A full understanding of solute transport begins with a knowledge of the above interactions.

Miscible Displacement

The term miscible displacement refers to the process of one fluid miscible with another invading and displacing the latter. With the fluids being miscible, they are able to completely mix, dissolve and dilute each other. Here after considering miscible displacement in a capillary tube without molecular diffusion, we progress to laboratory experiments displacing solutes having different kinds of soil that undergo various chemical and physical reactions. Simple theoretical concepts are used to explain the results. Our understanding of processes occurring during miscible dispacement will be illustrated in the lectures during the course with measurements of leaching and fertilizer movement in field soils.

In a Single Capillary without Diffusion

From the definition of viscosity, the velocity distribution of a liquid within a capillary tube of radius a during steady, uniform flow is derived to be the well-known parabolic velocity distribution

$$v(r) = 2v_o\left(1 - \frac{r^2}{a^2}\right) \tag{60}$$

where $v(0) = 2v_o$. The average velocity $\bar{v}$ of the liquid is v_o. Integrating $v(r)$ with the areal cross-section of the capillary, the volumetric flow rate Q ($cm^3 \cdot s^{-1}$) through the capillary is

$$Q = \frac{a^4 \pi \Delta P}{8\eta L} \tag{61}$$

If we rely solely on Eq. 60 to describe the fluid velocity, what will be the distribution of a second fluid of concentration C_o as it displaces a fluid of zero concentration initially within the capillary of length L? Assume that the solution C_o enters the tube at $x = 0$ at time $t = 0$. The concentration C averaged over the cross section of the capillary at distance x is

$$C_a = \frac{1}{\pi a^2}\int_0^a 2\pi r\, C(r)dr \tag{62}$$

or as a function of distance and time is

$$C_a(x,t) = C_o(1 - x/2v_o t) \tag{63}$$

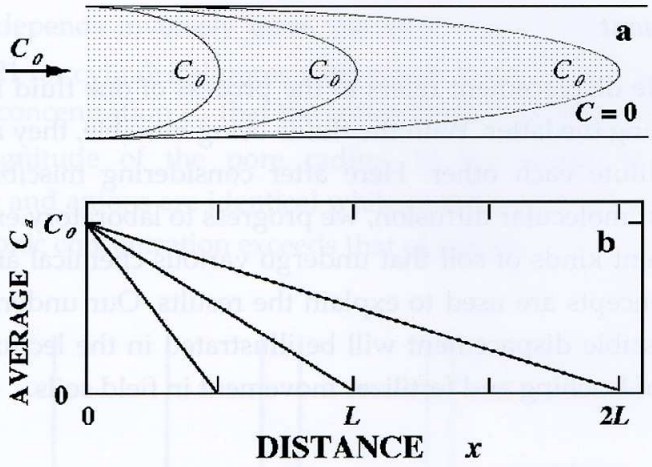

Fig. 22 - Parabolic velocity distributions of an invading solution C_0 within a capillary tube give rise to linear average concentrations along the tube (Eq. 63).

In Fig. 22, the paraboloid of the displacing fluid C_o within the capillary gives rise to a linear concentration distribution. When the invading front of C_o has reached a distance $2L$, the average concentration across the plane normal to the capillary at a distance of L is $C_o/2$. Interestingly, the average concentration of the fluid moving across the plane L at that instant is not $C_o/2$ but $3C_o/4$. The average concentration of fluid moving past $x = L$ (see Fig. 23a) is

$$C_a = \frac{mass\ of\ solute\ moving\ past\ x = L}{volume\ of\ fluid\ moving\ past\ x = L} \quad (64)$$

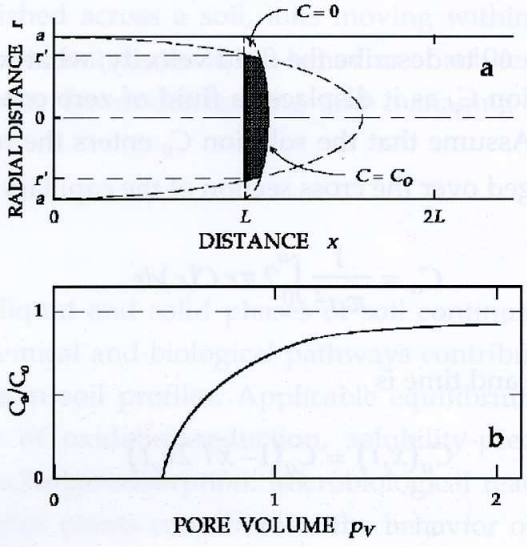

*Fig. 23 - **a.** Diagram of an elementary volume of liquid moving within a capillary tube. **b.** Average relative concentration of liquid leaving a capillary tube of length* L *as a function of pore volume (Eq. 66).*

Eq. 64 leads to

$$\begin{aligned} C_a(t)/C_o &= 0 && v_o t/L \le 0.5 \\ &= 1 - L^2/4v_o^2t^2 && v_o t/L > 0.5 \end{aligned} \tag{65}$$

or

$$\begin{aligned} C(p)/C_o &= 0 && p \le 0.5 \\ &= 1 - 1/4p^2 && p > 0.5 \end{aligned} \tag{66}$$

where $p = v_o t/L$ and is the ratio of the volume of fluid passing $x = L$ to the volume of the capillary between $0 \le x \le L$. Pore volume of effluent or simply pore volume is the name commonly used for p. The value of $C = 3C_o/4$ for $p = 1$ and approaches unity as $p \to \infty$, see Fig. 23b. Even for such a simple geometry as a capillary tube, the concentration distribution within the tube (Fig. 22b) is not easily reconciled with the shape of the concentration elution curve (Fig. 23b).

Convective Transport of Solutes

The spreading or dispersion of the solute caused by convective transport with the water can be qualitatively visualized in Fig. 24 for a simplified soil. The invading stream of solute partitions itself according to the microscopic pore water velocities occurring between the soil particles. At still a smaller scale, the water velocity is zero at the particle surface, departs markedly from the mean flow direction and approaches a zero value in the vicinity of dead-end pores. These pathways and pore water velocities, severely altered with slight changes of water content, have yet to be quantitatively evaluated. In the near future, computer-aided micro tomography and nuclear magnetic resonance techniques will provide an opportunity to ascertain the exact nature of the velocities at the pore scale.

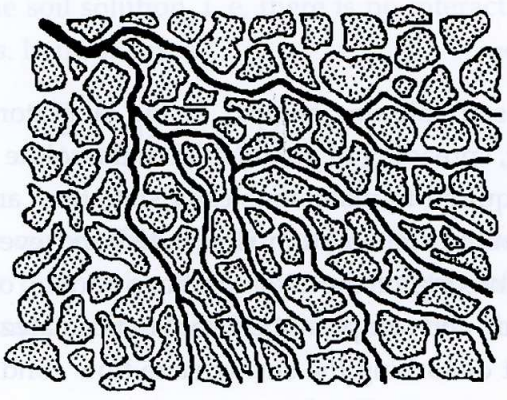

***Fig. 24** - Spreading or dispersion of a solute caused by convective transport in a simplified soil.*

For water infiltrating into a deep, homogeneous, water-saturated soil, we see in Fig. 25 that a solute of concentration C_o maintained at a point on the soil surface is dispersed vertically and horizontally. The velocity of the soil solution varies in both magnitude and direction owing to the distribution of irregularly shaped pores within the soil. Along transect A-A', the initial concentration C_o at $z = 0$ gradually diminishes to zero. Similarly, the concentration distribution normal to the average flow along transect B-B' gradually broadens with soil depth.

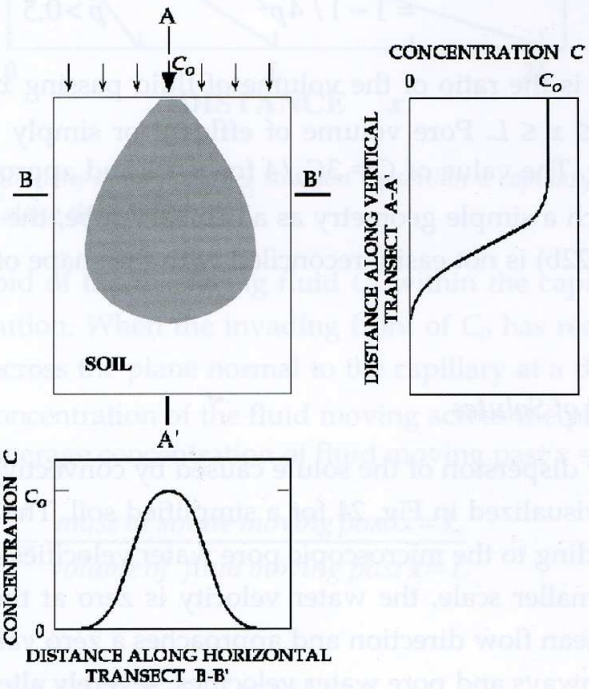

Fig. 25 - A solution of concentration C_o being introduced at one point on the surface of a uniform, water-saturated soil during steady state infiltration.

Laboratory Observations

One dimensional soil columns studied in the laboratory provide a simple means of quantifying the mixing, spreading or attenuation of the solute schematically presented in Fig. 25. An apparatus is required to maintain steady state flow and invariant soil water content conditions when the initial soil solution is invaded and eventually displaced by a second miscible solution. No mixing of the two solutions should occur at their boundary before entering the soil column, and samples of effluent to be analyzed for solute concentration has to be collected without disturbing the steady state flow conditions. A cross sectional sketch of a typical apparatus is given in Fig. 26.

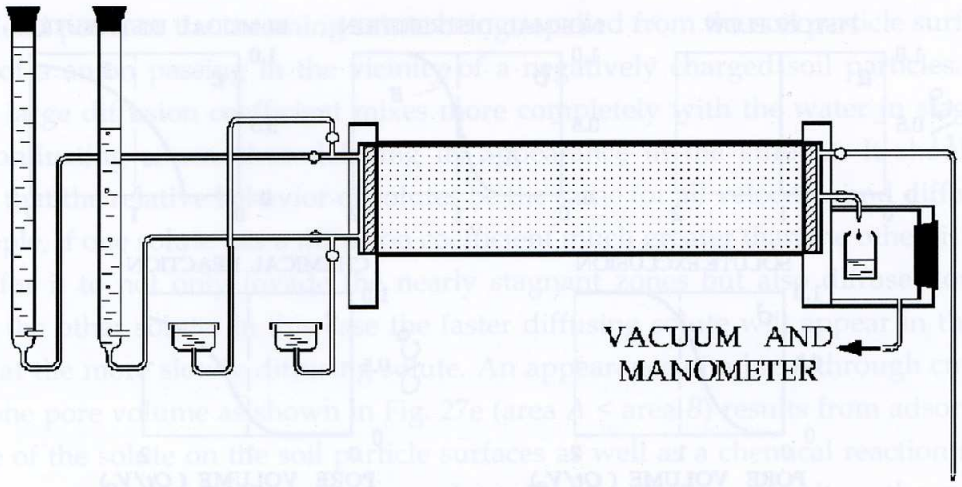

***Fig. 26** - Laboratory apparatus for conducting miscible displacement experiments with soil columns.*

Breakthrough Curves

Let the volume of the soil column occupied by soil solution be V_o and the rate of inflow and outflow of the soil solution be Q. If the initial soil solution identified by a solute concentration C_i is suddenly displaced by an incoming solution C_o, the fraction of this incoming solute in the effluent at time t will be $(C - C_i)/(C_o - C_i)$, or for an initial concentration of zero, simply C/C_o. Plots of C/C_o versus pore volume of effluent (Qt/V_o), commonly called breakthrough curves, describe the relative times taken for the incoming solution to flow through the soil column. Note that the definition of pore volume of effluent is not restricted to water-saturated conditions but is applicable to all soil water contents. Any experimentally measured breakthrough curve may be considered one or a combination of any of the five curves shown in Fig. 27.

For Fig. 27a-c, the solute spreads only as a result of molecular diffusion and microscopic variations of the velocity of the soil solution, i. e. there is no interaction between the solute, water and soil particle surfaces. In these cases

$$\frac{Q}{V_o}\int_0^\infty (1-C/C_o)dt = 1 \qquad (67)$$

regardless of the shape of the curve. This equation expresses the fact that the original soil solution occupied exactly one pore volume or that the quantity of solute within the soil column that will eventually reach a chemical equilibrium with that in the influent and effluent is C_oV_o.

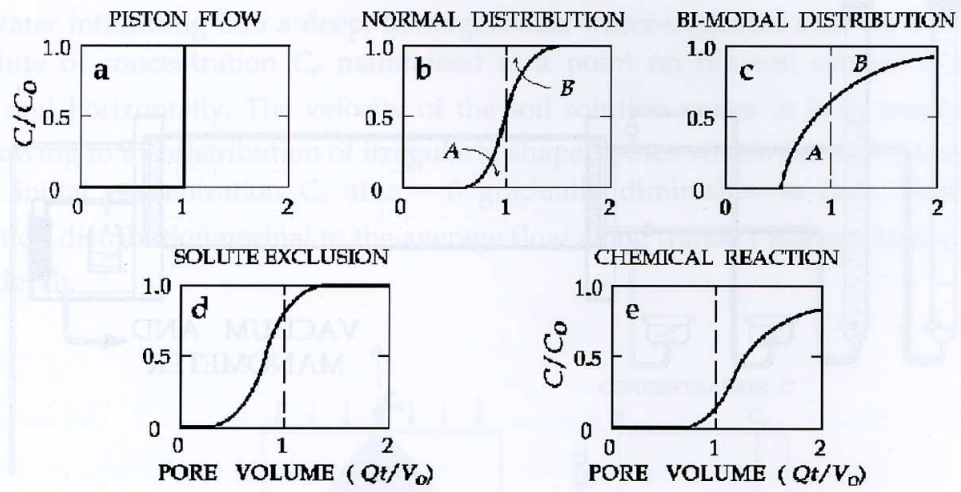

Fig. 27 - Types of breakthrough curves for miscible displacement. C/C_o *is the relative concentration of the invading fluid measured in the effluent and pore volume is the ratio of the volume of effluent to the volume of fluid in the sample.*

Note also that the area under the breakthrough curve up to one pore volume (area *A* in Fig. 27b and c) equals that above the curve for all values greater than one pore volume (area *B*), regardless of the shape of the curve. This latter statement is a direct result of Eq. 67, i. e.

$$\frac{Q}{V_o}\int_0^{V_o/Q}(C/C_o)dt = \frac{Q}{V_o}\int_{V_o/Q}^{\infty}(1 - C/C_o)dt \qquad (68)$$

Danckwerts (1953) defined holdback H_b as the left hand term of Eq. 68 having a range $0 \leq H_b < 1$ for non reacting solutes. The concept of holdback is a useful qualitative description whenever interactions between solute, water and soil solids are minimal. It indicates the amount of the soil water or solutes not easily displaced. Values of H_b for unsaturated soils have been evaluated to be 3 to 4 times greater than those for saturated soils.

Piston flow (Fig. 27a) never occurs owing to solute mixing that takes place by molecular diffusion and variations in water velocity at the microscopic level within soil pores. The breakthrough curve shown in Fig. 27b is characteristic of the longitudinal spreading of a solute as it is displaced through a soil having a normally distributed sequence of pores. Evidence for lack of solute-solid interaction is the fact that the areas *A* and *B* described by Eq. (68) are identical. A water-saturated soil composed of equal-sized aggregates manifesting a bimodal pore water velocity distribution typically yields the breakthrough curve given in Fig. 27c. With the areas *A* and *B* of this curve being comparable, any interaction between the solute and the soil particles is negligible.

An appearance of a breakthrough curve to the left of one pore volume as shown in Fig. 27d (area *A* > area *B*) results from the incoming solution not displacing water in stagnant

and deadend pores or the incoming solute being repelled from the soil particle surfaces as in the case of a anion passing in the vicinity of a negatively charged soil particles. A solute having a large diffusion coefficient mixes more completely with the water in stagnant and slowly conducting zones, thus delaying its appearance in the effluent. It should not be expected that the relative behavior of solutes be the same for all velocities and different soils. For example, if one solute has a diffusion coefficient much greater than the other, it would be possible for it to not only invade the nearly stagnant zones but also diffuse downstream ahead of the other solute. In this case the faster diffusing solute will appear in the effluent earlier that the more slowly diffusing solute. An appearance of a breakthrough curve to the right of one pore volume as shown in Fig. 27e (area A < area B) results from adsorption and exchange of the solute on the soil particle surfaces as well as a chemical reaction in the soil that serves as a sink for the incoming solute. Unsaturating a soil alters the pore water velocity distribution, allows some of the solute to arrive downstream earlier and increases the magnitude of holdback manifested by area A in Fig. 27. Desaturation eliminates larger flow channels and increases the volume of water within the soil which does not readily move. These almost stagnant water zones act as sinks to molecular diffusion. Later we shall discuss the opportunity afforded by controlling the water content and pore water velocity to change the leaching efficiency of field soils.

Theoretical Description

Several different kinds of theories have been proposed and equations derived to describe solute transport in both inert and reactive porous media. A comprehensive treatment would include transfers of the solute in all three phases of the soil – gas, liquid and solid. Here we consider the cornerstone of most theoretical descriptions – the convective-diffusion equation. Although it is commonly used to describe miscible displacement, it is nevertheless fraught with difficulties and approximations not easily resolved in the laboratory or the field.

We begin with a prism element having edges of length Δx, Δy and Δz. The difference between the mass of solute entering the prism and that leaving the prism equals the difference of the solute stored in the prism in time Δt providing that we account for any appearance (source) or disappearance (sink) of the solute within the prism by mechanisms other than transport. The solute flux density into the prism in the direction of the x axis is J_x. If we assume the change in J_x is continuous, the solute flux density out of the prism in the same direction is $[J_x + (\partial J_x/\partial x)\Delta x]$. The solute mass into the prism is $J_x\,\Delta y\Delta z\Delta t$ and that out of the prism is $[J_x + (\partial J_x/\partial x)\Delta x]\Delta y\Delta z\Delta t$. The difference between the mass into and out of the prism is

$$\{J_x \Delta y \Delta z \Delta t - [J_x + (\partial J_x / \partial x)\Delta x]\Delta y \Delta z \Delta t\} \tag{69}$$

or

$$-\left(\frac{\partial J_x}{\partial x}\right)\Delta x \Delta y \Delta z \Delta t. \tag{70}$$

Similar equations are derived for the directions of the y and z axes.The sum of the differences in three directions equals the change of the solute content of the prism. Provided that the total mass of solute associated with both the liquid and solid phases per unit volume of prism$S(t)$ has a continuous derivative for $t > 0$, we obtain the equation of continuity

$$\frac{\partial S}{\partial t} = -\left(\frac{\partial J_x}{\partial x} + \frac{\partial J_y}{\partial y} + \frac{\partial J_z}{\partial z}\right). \tag{71}$$

If we further take into consideration irreversible sources or sinks ϕ_i occurring within the prism during the time period over which the equation applies, we have

$$\frac{\partial S}{\partial t} = -\left(\frac{\partial J_x}{\partial x} + \frac{\partial J_y}{\partial y} + \frac{\partial J_z}{\partial z}\right) + \sum_i \phi_i. \tag{72}$$

In general, soil solutes exist in both gaseous and aqueous phases as well as being associated with the solid organic and inorganic phases of the soil. Here, we neglect the fact that non aqueous polar and non polar liquids can also reside in soils and participate in the displacement process. We have also assumed that the solutes in the soil solution are not volatile and have ignored their content and transport in the gaseous phase. Hence, the total solute concentration S in Eq. 72 is

$$S = \rho_T C_S + \theta C \tag{73}$$

where ρ_T is the soil bulk density, C_S the solute adsorbed or exchanged on the soil solids and C the solute in solution.

The solute flux density J in Eq. 72 relative to the prism $\Delta x \Delta y \Delta z$ is difficult to define unambiguously owing to the fact that the representative elementary volumes of each of the terms in J and S are not necessarily equal nor known, particularly for structured field soils. Each of the directional components of J is comprised of contributions of solute movement within the liquid phase as well as along particle surfaces of the solid phase. We assume that solute movement along soil particle surfaces is nil or can be accounted for by functions relating the concentration of solutes in solution to that associated with the solid phase in Eq. 73.

Hence, the solute flux density consists of two terms, one describing the bulk transport of the solute moving with the flowing soil solution and the second describing the solute moving by molecular diffusion and meandering convective paths within the soil solution. For the z-direction, we have

$$J_z = q_z C - \theta\left(D_{c_z} = D_{m_z}\right)\frac{\partial C}{\partial z} \tag{74}$$

where q_z is the Darcian soil water flux, D_{c_z} and D_{m_z} are the coefficients of convective dispersion and molecular diffusion in the soil solution, respectively. Equations for J_x and J_y are identical to Eq. 74 when z has been replaced by x and y, respectively. We continue the analysis here for only the vertical soil profile direction.

Substituting Eqs. 73 and 74 into Eq. 72, we obtain for a solute of the soil solution that does not volatilize into the soil air

$$\frac{\partial(\rho_T C_S)}{\partial t} + \frac{\partial(\theta C)}{\partial t} = \frac{\partial}{\partial z}\left[\theta\left(D_c + D_m\right)\frac{\partial C}{\partial z}\right] - \frac{\partial(qC)}{\partial z} + \sum_i \phi_i . \tag{75}$$

The first term of Eq. 75 describes the rate at which a solute reacts or exchanges with the soil solids. With $D_a = \left(D_c + D_m\right)$, Eq. 72 reduces to

$$\frac{\partial(\rho_T C_S)}{\partial t} + \frac{\partial(\theta C)}{\partial t} = \frac{\partial}{\partial z}\left(\theta D_a \frac{\partial C}{\partial z}\right) - \frac{\partial(qC)}{\partial z} + \sum_i \phi_i . \tag{76}$$

The source-sink term ϕ_i in Eq. 75 or Eq. 76 is often approximated by zero- or first-order rate terms

$$\phi_i = \gamma\theta + \gamma_s\rho + \mu\theta C + \mu_s\rho_T C_s \tag{77}$$

where γ and γ_s are rate constants for zero-order decay or production in the soil solution and solid phases, respectively, and μ and μ_s are similar first-order rate constants for the two phases. For radioactive decay, physicists may safely assume that μ and μ_s are identical as well as assuming that both γ and γ_s are nil. Microbiologists, considering organic and inorganic transformations of soil solutes in relation to growth, maintenance and waste metabolism of soil microbes as a Michaelis-Menten process, often simplify their considerations to that of ϕ_i in Eq. 77. McLaren (1970) provided incentives to study such reactions as functions of both space and time in soil systems – a task not yet achieved by soil microbiologists, especially when the individual characteristics of each microbial species is quantified and not lumped together as a parameter of the entire microbial community. Agronomic or plant scientists consider ϕ_i as an irreversible sink and source of solutes taking

place in the vicinity of the rhizosphere of cultivated or uncultivated plants as a function of soil depth and time as well as some empirical function defining the root distribution.

For a solute that does not appreciably react with the soil particles, does not exist in the soil air and does not appear or disappear in sources or sinks, respectively, Eq. 76 reduces to

$$\frac{\partial C}{\partial t} = \frac{\partial}{\partial z}\left(D_a \frac{\partial C}{\partial z} \right) - \frac{\partial (vC)}{\partial z} \tag{78}$$

For steady state flow in a homogeneous soil at constant water content, Eq. 78 reduces still further to

$$\frac{\partial C}{\partial t} = D_a \frac{\partial^2 C}{\partial z^2} - v \frac{\partial C}{\partial z} \tag{79}$$

which has been extensively used to develop empirical relations between the apparent diffusion coefficient D_a and the average pore water velocity v.

Numerical and analytical solutions for the above equations subject to specific initial and boundary conditions are available.

Theoretical Implications

The majority of inorganic cations, anions and solutes in soil solutions have diffusion coefficients in the order of 10^{-5} $cm^2 \cdot s^{-1}$ while organic cations, anions and solutes usually manifest much smaller values. These coefficients are moderately temperature dependent and slightly concentration dependent. The importance of their different magnitudes is apparent only at relatively small pore water velocities.

The existence of concentration gradients of inorganic salts in the soil solution responsible for solute transfer by diffusion or as a result of convection guarantees that the displacing and displaced solutions do not generally have identical values of density or viscosity no matter how close their values. In soils, it is not uncommon to experience solutions of unequal density and viscosity. During the extraction of water from soil profiles by plants or by evaporation at the soil surface, the density and viscosity of the soil solution increase continually. Conversely the infiltration of rain or many irrigation waters causes the soil solution to be diluted. Fertilizers and other agrochemicals also alter these properties of the soil solution. The density and viscosity of the soil solution also differ from those of the bulk solution owing to the interaction of water and the soil particle surfaces especially in unsaturated soils or those soils having large clay contents.

Although arid soils usually are dominated by constant charge colloids and tropical soils by those of constant potential, all soils are mixtures of both, and hence pH cannot be ignored. For soils containing substantial amounts of clay having a variable surface charge, the pH will depend upon solute concentration. For such soils differences in leaching characteristics are a result of the concentration of the soil solution rather than strictly being caused by hydrodynamic and geometric aspects of the flow regime.

The mixing and attenuation of a solute by convection depend upon the pore size distribution and the number of bifurcations experienced by the soil solution as water flows through its system of microscopic pores (recall Fig. 24). The greater the total macroscopic displacement length, the greater will be the opportunity for both convective and diffusive mixing. As the displacement length increases, both the number of bifurcations in the pore system and the time for molecular diffusion increase. Hence the deeper the displacement, the greater is the spreading of the solute.

Soil and Water Management Implications

Although our understanding and theoretical description of solute transport in soils remain incomplete, we have nevertheless sufficient knowledge to derive a few principles or guidelines for managing solute retention or leaching in the field. Whether solutes accumulate or leach depends primarily upon the processes by which they enter, react and leave the soil profile relative to their association with water. Here, we disregard horizontal surface and subsurface water flow, and focus our attention on transport owing to the water content and flux density conditions at the soil surface occurring naturally owing to local weather conditions and being deliberately modified by irrigation.

Summarizing the more important points of this chapter, we conclude the following regarding the relative movements of soil water and its dissolved constituents:

a) As water moves more slowly through a soil, there is a greater opportunity for more complete mixing and chemical reactions to take place within the entire microscopic pore structure owing to the relative importance of molecular diffusion compared with that of convection.

b) Microscopic pore water velocity distributions manifest their greatest divergence for water-saturated soil conditions. Hence, under water-saturated conditions, the greatest proportion of water moving through the soil matrix occurs within the largest pore sequences.

c) Under water-saturated soil conditions, when the average pore water velocity is large compared with transport by molecular diffusion, the relative amount of solute being displaced depends upon the solute concentration of the invading water.

d) The concept of preferential flow paths occurs at all degrees of water-unsaturation even though their existence is usually only demonstrated for macropores near water-saturation. At each progressively smaller water content, the larger pore sequences remaining full of water establish still another set of preferential flow paths.

e) Any attempt to measure the solute concentration based on extraction methods carried out either in the laboratory or the field will be dependent upon the rate of extraction and the soil water content during the extraction process.

f) Inasmuch as rainfall infiltration usually occurs at greater soil water contents and greater average pore water velocities than does evaporation at the soil surface, the amount of solutes transported near the soil surface per unit water moving through the soil surface is greater for evaporation than for infiltration.

Each of the above six points is verified by field experiments and published in numerous publications.

REFERENCES

Danckwerts P.V. (1953). Continuous flow systems. *Chem. Eng. Sci.* 2:1-13.

Iwata S., Tabuchi T. and B.P. Warkentin. (1988). Soil Water Interactions. M. Dekker, New York and Basel.

Jackson, R.D. (1964). Water vapor diffusion in relatively dry soil I. *Soil Sci. Soc. Am. Proc.* 28:172-176.

Kutílek M. and Nielsen D.R. (1994). Soil Hydrology. Catena Verlag, Cremlingen-Destedt, Germany.

McLaren A.D. (1970). Temporal and vectorial reactions of nitrogen in soil: A review. *Can. J. Soil Sci.* 50:97-109.

Richards L.A. (1965). Physical condition of water in soil. In: C.A. Black (Ed.): Methods of Soil Analysis, Part 1, Physical and Mineralogical Properties, Agronomy Monograph Series No. 9, ASA, Madison, p. 128-152.

Srinilta S.A., Nielsen D.R. and Kirkham D. (1969). Steady flow of water through a two-layer soil. *Water Resour. Res.* 5:1053-1063.

Takagi S. (1960). Analysis of the vertical downward flow of water through a two-layered soil. *Soil Sci.* 90:98-103.

Willis W.O. (1960). Evaporation from layered soils in the presence of a water table. *Soil Sci. Soc. Am. Proc.* 24:239-242.